Design criteria for a space-efficient sled capable of simulating different automatic emergency braking acceleration pulses.

Bhagawath Raj Thangavel[1,2], Thomas Seacrist[1], Valentina Graci[1,2]
[1]Center for Injury Research and Prevention, Children Hospital of Philadelphia, Philadelphia, USA
[2]School of Biomedical Engineering, Science and Health Systems, Drexel University, USA

ABSTRACT

Reproducing automatic emergency braking (AEB) maneuvers in laboratory settings, where weather and vehicle geometries are controlled, is advantageous for repeatably and safely quantifying occupant kinematics across different AEB pulses. The aim of this study is to design a space-efficient centrifuge sled that converts rotational acceleration into linear acceleration to reproduce different AEB pulses. To this scope, three design criteria were evaluated: a mathematical model, torque requirement and installation of the sled propulsion system, and wheel assembly for the sled rotation. The designed centrifuge sled consists of an arm rotating, and an occupant compartment turning as the centrifuge arm aligns the occupant in the direction of the resultant acceleration, so that the occupant experiences only linear forward acceleration. A mathematical model was created to compare the AEB pulse generated by the sled and a target AEB pulse. Cross-correlation was used to test the similarity of the two AEB pulses. The inertia, torque, and power of each sled component were calculated to select the appropriate propulsion system. An anchoring system consisting of an aluminum base plate secured the centrifuge servomotor to the ground was designed. A wheel assembly to support a minimum load of 300 Kg on each extremity of the centrifuge arm while maintaining maximum contact with the ground was also created. The similarity of the simulated and target AEB was high (R=0.9). The resulting centrifuge sled components' inertia, torque, and power equal to 984 kgm^2, 5530 Nm, and 30 kW respectively. Therefore, a servomotor with a maximum operating torque of 7060 Nm and power of 66 Kw was selected. The wheel assembly designed resulted to be able to handle maximum load 680 kg. These design criteria suggest that a rotational sled design to reproduce AEBs in the laboratory is feasible.

INTRODUCTION

AEB presence in the modern fleet have been proven to be effective in reducing collision rates (Cicchino et al., 2019). AEB pulses can vary significantly between different vehicle make and models (Graci et al., 2021). Variations in pulse characteristics can influence occupant kinematics during braking leading to a potential variety of occupant out-of-position postures. It is unclear how occupant motion is affected by the differences in AEB pulse characteristics. Some previous studies have attempted to simulate AEB both in the laboratory and via Finite Element (FE) simulations to understand occupant kinematics. However, the pulse characteristics were not within the boundaries of AEB pulses from real vehicles (Graci et al., 2021). For instance in (Kang et al., 2021)), the AEB pulses exhibited peak accelerations up to 0.8 g and ramp-time of 60 ms. However an AEB pulse

This paper is a student paper from the 20th Injury Biomechanics Symposium and is published in a special issue of SAE International Journal of Transportation Safety.
It is preliminary work, has not been peer reviewed, and should not be cited because it is a work in progress.

has a minimum ramp-time around 150ms (Graci et al., 2021). (Chan et al., 2022) used an AEB pulse with a 1 g peak acceleration and a jerk around 58 g/s. Both jerk and ramp-time were respectively were outside the range of a real-world AEB pulses (Graci et al., 2021). (Soni et al., 2023) used an AEB pulse with a 1 g peak acceleration and a ramp-time of 100 ms, which is again too short compared to real-world AEB pulses (Graci et al., 2021).

To recreate realistic AEB pulses, a long linear sled would be needed. For instance, the IIIHS conducted AEB tests with vehicles starting the approach phase of an obstacle between 75-105 m away (IIHS Test protocol 2024). Reproducing a 75 m sled in a laboratory could be impractical because of space constraints and costs. It is plausible that with the appropriate propulsion system, a shorter length sled could be built to reproduce an AEB pulse, but space would still potentially be an issue, or the sled would not be capable to reproduce a wide range of AEB pulses with a shorter length (Klug et al., 2024). Performing AEB test on a test-track with different vehicles to reproduce different AEB pulses present other challenges: different vehicles have different interior geometries that represents a confounding factor when comparing the effect of different AEB pulses, testing conditions are hard to control across tests (e.g. temperature, lighting, road surface, weather conditions can change between tests), costs of test-track rental and logistic of track-track use can be prohibitively expensive.

Compared to a test track, AEB tests can be conducted more repeatably in a laboratory setting, which is crucial because the effect of the AEB pulse characteristics on occupant kinematics needs to be isolated from any confounding factors (e.g. vehicle geometry, test driver variability, and road conditions). Therefore, a rotational sled concept was explored, and the aim of this study was to establish the design criteria for a rotational sled, hereafter referred to as "centrifuge sled". A centrifuge-based sled system can overcome space constraints by converting rotational motion into linear acceleration to replicate AEB pulse characteristics within a compact testing setup.

METHODS

Mathematical model of the centrifuge sled

The centrifuge sled in our study was designed as follows: a centrifuge arm rotates with a velocity and an occupant compartment that turns as the centrifuge arms rotates and aligns the occupant in the direction of the resultant acceleration (a(t) (red arrow, Figure 1). Consequently, an occupant would experience a linear acceleration, as in a vehicle undergoing automatic emergency braking. The counterweights placed on the other end of the centrifuge arm cancels the centrifugal force vector at the occupant-compartment which is due to the rotation of the centrifuge arm. In Figure 1, the top row depicts the schematic of both the centrifuge and the directions of the force vectors with respect to the bottom row that depicts the different phases of an ideal AEB pulse.

This paper is a student paper from the 20th Injury Biomechanics Symposium and is published in a special issue of SAE International Journal of Transportation Safety.
It is preliminary work, has not been peer reviewed, and should not be cited because it is a work in progress.

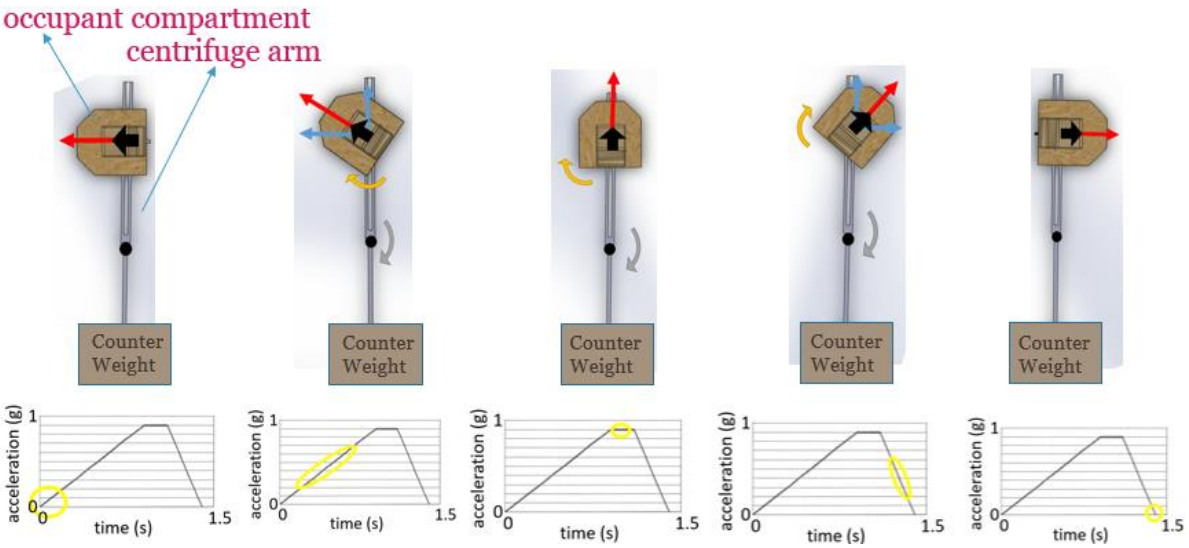

Figure 1. schematic of the centrifuge sled during different phases of the representative AEB pulse

A mathematical model was created to find the theoretical speed required to simulate a representative AEB pulse with a peak acceleration of 1g (Figure 1, bottom row) with the following parameters (Figure 2):

- $\omega(t)$ is the angular velocity of the centrifuge arm,
- $\emptyset(t)$ is the angular position of the occupant compartment,
- r (1.8 m) is the distance of the occupant compartment from the center of the centrifuge arm,
- $\omega'(t)$ is the angular acceleration of the centrifuge arm,
- The rotational acceleration vector component of the centrifuge arm is given by $a_c = r * \omega(t)^2$.
- The tangential acceleration vector component of the occupant compartment is given by $a_t = r * \omega'(t)$.
- The resultant acceleration vector of the occupant compartment corresponds to the linear forward acceleration experienced by the occupant (i.e. red arrow Figure 2) and it is calculated using the Pythagorean theorem: $a(t) = r\sqrt{(\omega(t))^4 + (\omega'(t))^2}$.

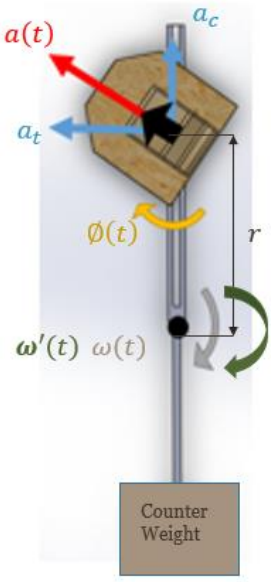

Figure 2. Free body diagram of the centrifuge sled.

$\emptyset(t)$ is a directional component that ensures that the occupant experiences linear acceleration only. In the equation below $\omega'(t)$ the AEB pulse acceleration of the centrifuge arm is considered the output parameter of the mathematical model. The resultant acceleration $a(t)$ is the target AEB pulse acceleration and can be considered as the input parameter while the velocity of the centrifuge arm $\omega(t)$ is the control parameter. To test our mathematical model, we reproduced $\omega'(t)$ by using the acceleration profile of a representative AEB pulse (i.e. Figure 1 bottom row, $a(t)$) as the input and by changing the values of $\omega(t)$.

This paper is a student paper from the 20th Injury Biomechanics Symposium and is published in a special issue of SAE International Journal of Transportation Safety.
It is preliminary work, has not been peer reviewed, and should not be cited because it is a work in progress.

$$\omega'(t) = \sqrt{(\frac{a(t)}{r})^2 - (\omega(t)^4)}$$

A custom MATLAB script integrated $\omega'(t)$ using the 4th order Runge-Kutta iterative method and the theoretical angular speed and acceleration was used to reproduce the AEB pulse. A cross-correlation between the representative AEB signal with the simulated AEB signal to evaluate how well the simulated AEB matches the generic realistic AEB was performed.

Centrifuge propulsion system torque requirements and installation.

To evaluate the required power of the drive system based on the mass and position of the rotating components of the centrifuge sled, a torque analysis was done to select a propulsion system on the market. The factors considered for the calculation of the torque of the propulsion system were the moment of inertia and acceleration of the system. The moment of inertia was assumed to be dominated by the primary masses in the system: the centrifuge arm, the occupant compartment, the counterweights, the occupant-compartment servomotor and gear box, seat, wheel assemblies, and system friction. Masses and the radius of the primary mass components from the axis of rotation were used to calculate the moment of inertia, (Table 1).

Table 1: Factors considered for torque distribution of the primary masses.

Factors considered for torque distribution		
Primary mass component	**Mass 'M' (kg)**	**Radius 'r' (m)**
Occupant compartment	24.5	1.8
Seat	15.4	1.8
Occupant	100	1.8
Counterweight	95.25	1.54
Occupant compartment servomotor	18.5	1.8
Occupant compartment Gearbox	20.4	1.8
Centrifuge arms	63.39	NA
Wheel Assembly	18.14	2
TOTAL	356.28	NA

Assuming that the minor masses such as the mass of fasteners are negligible, the masses and radius of the primary masses from the axis of rotation (Table 1) were used to calculate:

- The moment of inertia 'I' using the formula, $I = M * r^2$.
- The angular acceleration '$\omega'(t)$' by setting target maximum tangential acceleration a_t to 1g \ 9.8 m/s^2 and using the formula $a_t = r * \omega'(t)$.
- The torque contributions of the individual mass were in turn calculated using the previously calculated angular acceleration and the formula $\tau = I * \omega'(t)$.
- The power of the motor was calculated using the formula $P = \tau * \omega(t)$.

This paper is a student paper from the 20th Injury Biomechanics Symposium and is published in a special issue of SAE International Journal of Transportation Safety.
It is preliminary work, has not been peer reviewed, and should not be cited because it is a work in progress.

To install a propulsion system with a high torque capacity in the ground of our laboratory we had to design a mounting that increased the area of contact of the motor flange with the ground to dissipate any vibration caused by the centrifuge motor (Figure 3). We designed an aluminum base plate with a diameter of 1400mm and thickness of 15mm. Aluminum is a soft material compared to steel (motor flange material), so that an aluminum base plate would absorb any vibrations while increasing the anchoring area of the motor with the ground. Twelve "half-inch grade 5" bolts were selected to anchor the centrifuge motor and aluminum base to the ground. To obtain the maximum anchoring force of the anchoring design, the sheer strength of each bolt used to mount the flange and aluminum base to the ground plate was calculated by summing the sheer strength of each "half-inch grade 5" bolt, which was approximately 70,000psi. The anchoring force of each bolt was calculated as shear force = shear strength × cross sectional area. The resisting torque of the aluminum base was calculated as resisting torque = anchoring force × anchoring radius.

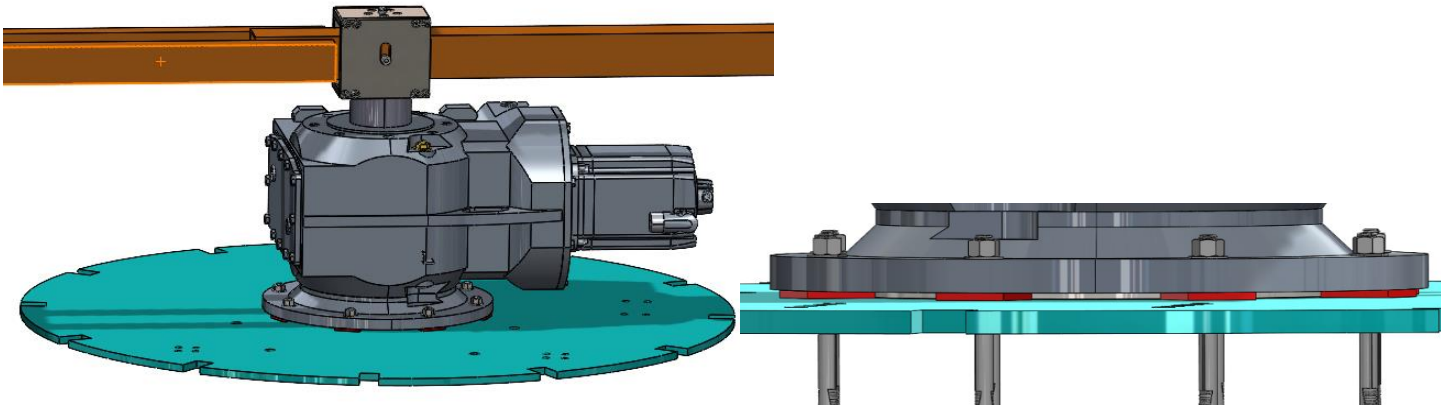

Figure 3. Centrifuge motor mounting (left), Aluminum base plate and spacers bolted to centrifuge servomotor flange (right)

To connect the centrifuge motor to the centrifuge arm, a pivot assembly was designed using stainless steel (Figure 4, left). The base of the pivot assembly was designed to be bolted to a shaft at the center of the centrifuge motor and the centrifuge arm. The cross-sectional view of the pivot assembly (Figure 4, middle) shows how the pivot assembly was connected to the center of the centrifuge arm with a jack screw at the center of the pivot assembly. The jack screw can also be used to lift the centrifuge arm upwards for the maintenance of the centrifuge sled in the future. The centrifuge motor generated torque would be transmitted to the centrifuge arm through a fabric reinforced rubber drive pads that allow free movement of the arm for balancing and bearing the load under operation (Figure 4, right).

This paper is a student paper from the 20th Injury Biomechanics Symposium and is published in a special issue of SAE International Journal of Transportation Safety.
It is preliminary work, has not been peer reviewed, and should not be cited because it is a work in progress.

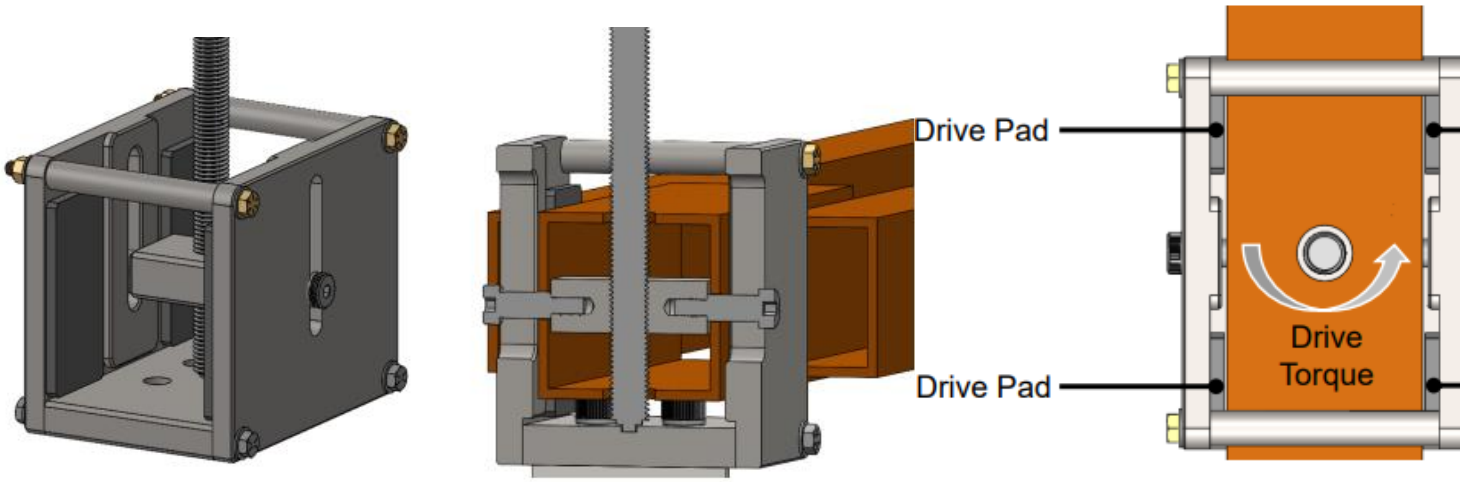

Figure 4. Pivot assembly design (left), Cross-sectional view of the pivot assembly attached to the centrifuge arm along with the jack screw (middle), Top view of the pivot assembly with rubber drive pads (right).

Wheel assembly design

To support the centrifuge arm at the two extremities a wheel assembly was designed consisting of 4 wheels and a suspension assembly attached to a cross bar (Figure 5, left). Three dampers were used to connect the centrifuge arm to the cross bar. The wheels and suspension design were created considering the following factors: the suspended weight of half of the centrifuge arm, the weight of the occupant compartment, the weight of a 100 kg occupant and the weight of the occupant compartment servo motor (weight values reported in Table 1). The total weight suspended on tires was assumed to be approximately 200 kgs on each side of the centrifuge arm. The tires selected for the design of wheel assembly were go-kart tires, which were preferred because of their maximum load rating of 170 kg under 14 psi pressure. The selected go-kart tire sizes for our wheel assembly have a small diameter (11 inches) and a high contact patch (5 inches). side view, top view and front view of the wheel assembly is reported in Figure 5 and 6. We design and mount the wheel assembly of the centrifuge by modelling the wheel hub bearing flange employed in front wheel steering in go-kart vehicles. This was done due to the steering knuckle spindle present in go-kart front wheel hubs. Both right and left wheels are locked using the steering knuckles of the wheel hub and a yellow-colored metal bracket (Figure 5, right). This kind of connection reduces the degree of freedom of movement for individual wheels in the axial direction and allows for the self-alignment of the tires while they rotate. Therefore, it can counteract any side slip angle produced in the wheels during the rotation of the centrifuge sled.

This paper is a student paper from the 20th Injury Biomechanics Symposium and is published in a special issue of SAE International Journal of Transportation Safety.
It is preliminary work, has not been peer reviewed, and should not be cited because it is a work in progress.

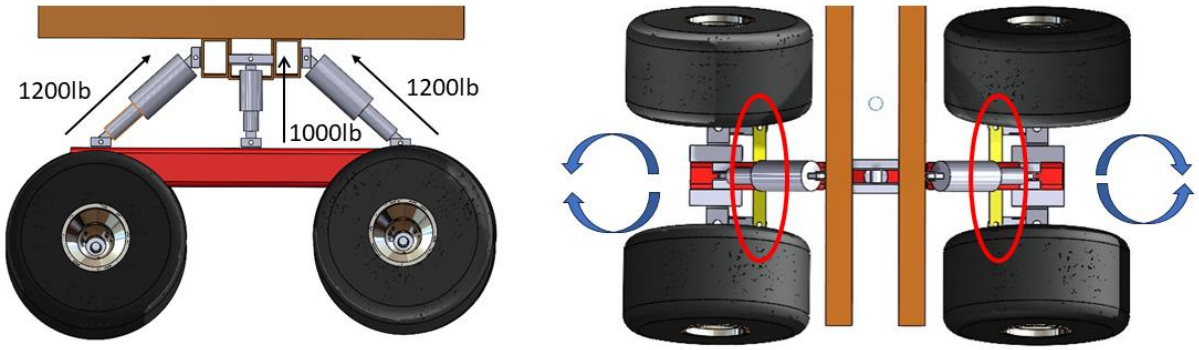

Figure 5. Side view of wheels and suspension assembly with maximum load rating of each damper (left), Top view of the wheel assembly with both the wheel's steering spindle connected as marked (right)

Camber is an alignment setting of a car's wheels that refers to the tilt of the car's wheel relative to the vertical axis when viewed from the front or rear of the vehicle. It's a key alignment setting that affects handling, tire wear, and stability. Camber is positive if the top of the wheel tilts outward or negative if the top of the wheel tilts inward. In our wheel assembly, we selected a negative camber angle for our tires to maximize tire contact with the ground during cornering (Figure 6). Therefore, the wheel hubs were designed with a negative camber angle of 10 degrees so that when the centrifuge sled rotates in a circular direction, the camber angle would improve tire contact with the ground and stabilize the whole centrifuge sled. Figure 6 shows the contact patch and normal force vectors F_n acting on the wheel assembly from the front view. In idle condition the force vectors would converge from the contact patches between tires and ground towards the damper. When the centrifuge sled is rotating, the centrifugal force vector F_c pushes the normal force vectors F_n outward and increases the contact patch of the tire.

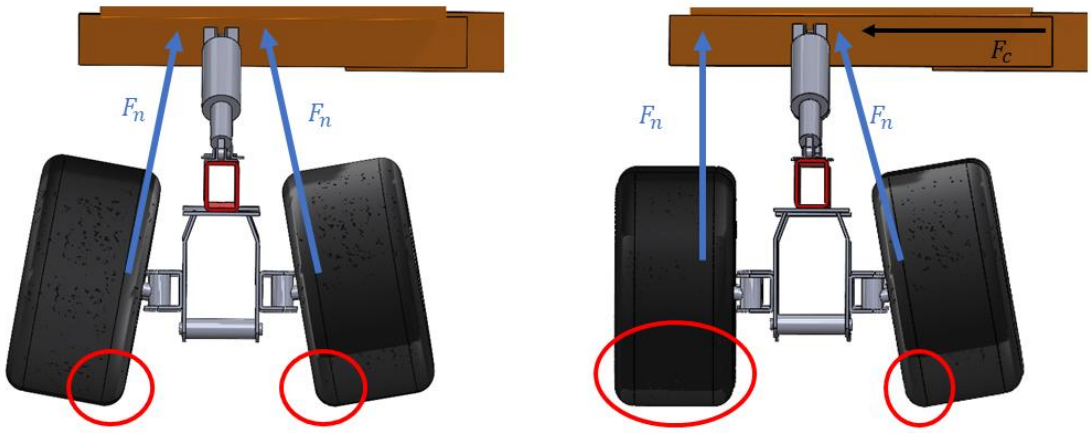

Figure 6. Contact patch and force vectors due to camber when the system is idle(left) and rotating (right)

This paper is a student paper from the 20th Injury Biomechanics Symposium and is published in a special issue of SAE International Journal of Transportation Safety.
It is preliminary work, has not been peer reviewed, and should not be cited because it is a work in progress.

RESULTS

The output of our mathematical model validated that the theoretical angular speed and angular acceleration required at the peak of the AEB acceleration pulse was approximately 13 degrees per second and 33 degrees per second squared respectively (Figure 7, right). The output plots of the mathematical model (Figure 7, left) in the ramp-up phase showed that, the simulated acceleration profile $\omega'(t)$ successfully followed the target acceleration profile a(t) reproducing an AEB pulse in the ramp-up phase and around acceleration, which are the most relevant phases of the AEB pulse for the occupant kinematics (i.e. peak head excursion occurs around peak acceleration). The cross-correlation plots reported in Figure 7 represent the representative AEB signal $a(t)$ and the simulated AEB signal $\omega'(t)$. The cross-correlation coefficient of 0.99 showed that a strong similarity between the two AEB signals, suggesting that the theoretical working principle of the centrifuge sled was valid.

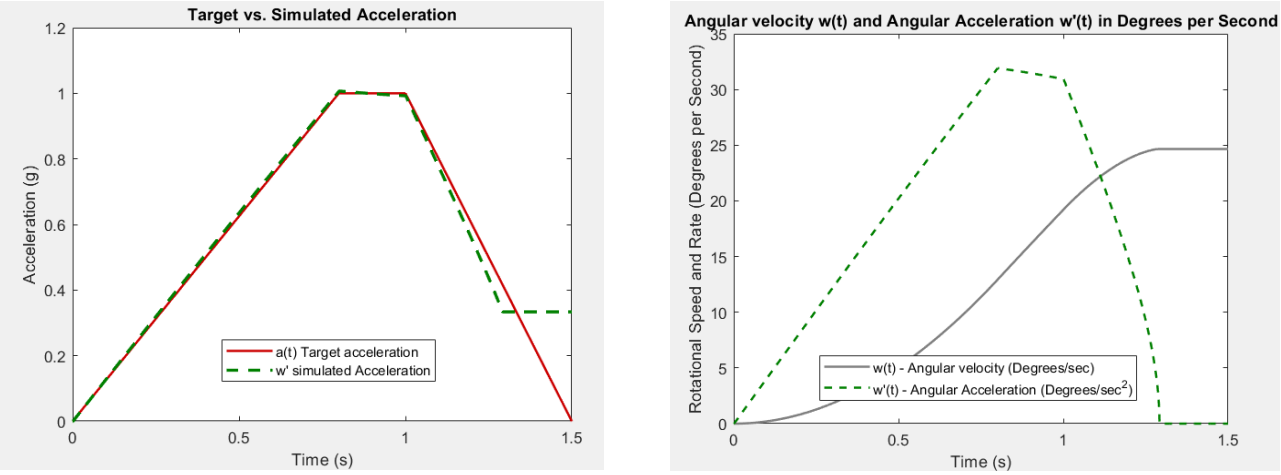

Figure 7. Target AEB pulse a(t) vs simulated AEB pulse $\omega'(t)$ (left), Angular velocity $\omega\ (t)$ and angular acceleration $\omega'(t)$ of the centrifuge arm (right)

A limitation of our theoretical mathematical model was the assumption that the inertia of the system was negligible. Therefore, it was necessary to consider the inertia of the physical masses rotated by the centrifuge sled to calculate the torque requirements of the main propulsion system. The moment of inertia and torque calculated for the individual primary masses of the sled are reported in Table 2. The cumulative torque and power requirements calculated for the centrifuge sled was 5540 Nm and 30 kW respectively. The torque contributions of the individual primary masses are reported in Figure 8. To account for the required power and positional accuracy to reproduce realistic AEB pulses, a servomotor was selected with a maximum torque and power rating of 7060 Nm and 66 kW respectively. Using the maximum torque of the selected centrifuge servomotor the maximum load capacity at 1.8 m radius was calculated to be 400kg.

This paper is a student paper from the 20th Injury Biomechanics Symposium and is published in a special issue of SAE International Journal of Transportation Safety.
It is preliminary work, has not been peer reviewed, and should not be cited because it is a work in progress.

Table 2: Moment of inertia and torque required for the primary masses of the Centrifuge sled.

Torque distribution		
Primary mass component	**Moment of inertia 'I' (kg*m^2)**	**Required Torque 'τ' (Nm)**
Occupant compartment	79.38	432.18
Seat	49.89	271.65
Occupant	324	1764
Counterweight	228.67	1244.99
Occupant compartment servomotor	59.94	326.34
Occupant compartment gearbox	66.1	359.85
Centrifuge arms	103	560.78
Wheel Assembly	72.57	395.12

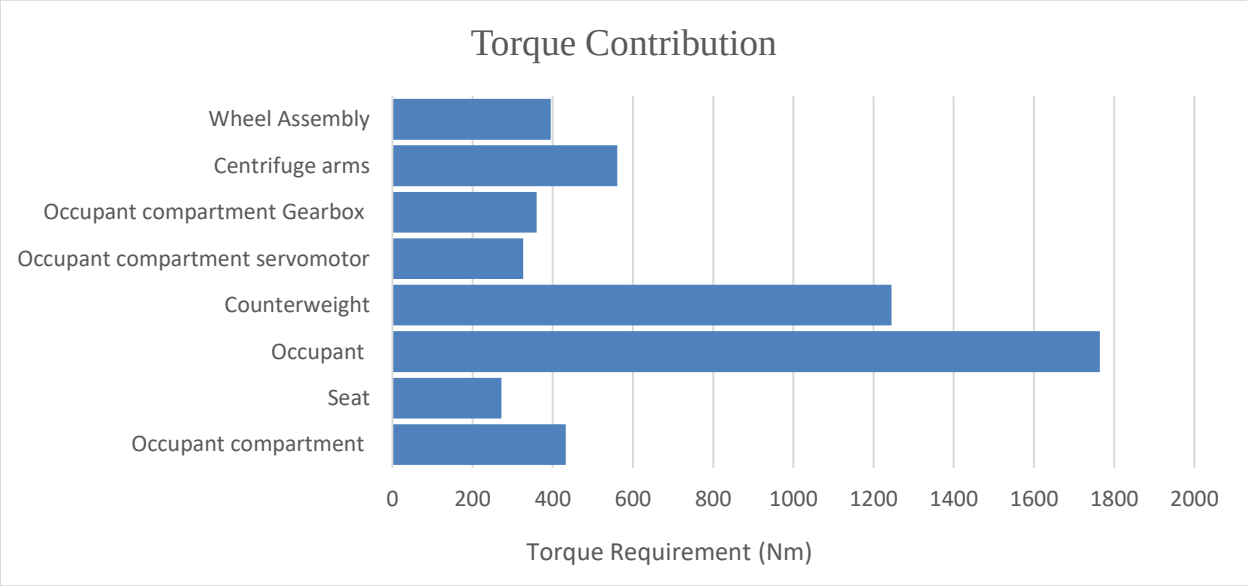

Figure 8. Torque contribution by different components of the centrifuge sled.

The selected high torque capacity propulsion system had a flange of 450 mm in diameter so that the selected aluminum base plate diameter (i.e. up to 1400 mm) for installation, increased the motor anchoring area significantly. The cumulative sheer strength of the 12 bolts used to anchor both the centrifuge servomotor and the aluminum base plate to the ground was 12 × 70,000psi = 840,000psi. Consequentially, the total shear strength (840,000psi) multiplied by each bolt cross sectional area (0.196 in²) is equal to the shear force (164,640 lbs). To calculate the resistive torque that the anchoring system can withhold, the anchoring force was converted to newtons using 160,000 lbs = 160,000×4.44822 ≈ 711715.2 N. The anchoring radius of the anchoring system is 700 mm (i.e. 0.7m). Therefore, the resulting total resisting torque of the anchor aluminum baseplate is equal to 711,715.2 × 0.7 = 498,200.64 Nm.

This paper is a student paper from the 20th Injury Biomechanics Symposium and is published in a special issue of SAE International Journal of Transportation Safety.
It is preliminary work, has not been peer reviewed, and should not be cited because it is a work in progress.

The maximum load rating of the selected dampers was used to calculate the maximum permissible load on the damper system. Figure 5 depicts the maximum permisible load rating on each damper, using trignometry the maximum permisible load that can be suspended on the damper system was calculated to be 3400 lbs or 1542 kgs for each end of the centrifuge arm. However, since the tires are the part of the machine that is in contact with the ground, the maximum load rating of the tires would be considered as the maximum load rating the centrifuge sled can support. Each selected tire has a load rating of 170kg. Since each end of the centrifuge sled has four such tires for support, the cumulative load rating is 680kg. However, since the servomotor can handle up to 360kg at 2m radius from the axis of rotation, 360 kg will be currently considered as the maximum load the centrifuge sled can propel.

DISCUSSION

The mathematical model validated the theoretical working principle of the capacity of a rotational sled to reproduce an AEB pulse. The overlap between the resulting AEB acceleration profile from the model and the representative AEB pulse depicted in Figure 7 showed that it is theoretically possible to simulate a linear AEB pulse using angular velocity and angular acceleration with a rotational sled.

The mathematical model has two shortcomings. First, the equation $\omega'(t) = \sqrt{(\frac{a(t)}{r})^2 - (\omega(t)^4)}$ does not allow negative values of angular acceleration, since $\omega'(t)$ is the result of a square root. This is the reason why the simulated AEB acceleration $\omega'(t)$ did not follow the target acceleration $a(t)$ in the ramp down phase of the pulse (Figure 7, left). This can also be observed in the plot (Figure 7, right) showing that the angular velocity of the centrifuge arm drops to zero, while the angular acceleration of the centrifuge arm remains constant. Second, the equation does not account for any inertia of the centrifuge sled caused due to rotation. These limitations can be overcome during testing by using a Proportional Integral Derivative controller to fine tune the servomotor rotation in real time and can be calibrated to produce an AEB pulse. Furthermore, the occupant compartment rotation is now controlled by an occupant-compartment servomotor, that is placed under the occupant compartment. The occupant compartment is currently a work in progress and therefore has not been included in this study. The occupant-compartment servomotor would be controlled by a feedback loop to the PID controller that controls the centrifuge servomotor rotation and sync it to the occupant compartment rotation in real time. The feedback loop would allow the sled system to self-adapt and control the position and speed of both servomotors such that the occupant experiences only linear acceleration during the AEB simulation.

The maximum torque rating of the selected centrifuge servomotor was 7060 Nm which was greater than the calculated operating torque 5540 Nm of the centrifuge sled. The greater torque capacity of the selected centrifuge servomotor provides a margin of safety as well as make modifications to the occupant compartment or any other primary mass components of the system. The resisting torque of 498,200 Nm for the aluminum base design suggests that an equivalent magnitude of torque is required for the anchoring mount design to fail and dislodge the servomotor from the ground. However, both the maximum torque capacity of the selected servo motor (i.e.

This paper is a student paper from the 20th Injury Biomechanics Symposium and is published in a special issue of SAE International Journal of Transportation Safety.
It is preliminary work, has not been peer reviewed, and should not be cited because it is a work in progress.

7060 Nm) and the required operating torque for our sled application (5540 Nm) represent around 2% of the resisting torque generated by the anchoring system suggesting that our motor will be secured without dislodging risk in the ground of the laboratory.

Some previous laboratory-based sled used for reproducing pre-crash maneuvers (Arbogast et al., 2009) , (Holt et al., 2020) were equipped with rails on which the occupant compartment would move. Our sled has been designed with a wheel assembly, which have advantage to potentially reproduce the vertical component of the braking acceleration and the resulting pitch of the occupant compartment. Although pitch during an AEB event may have a negligible effect on the occupant, the wheel assembly may improve the similarity between our lab-based reproduction of an AEB and a vehicle AEB. Our wheel assembly was designed with a negative camber angle to ensure the support of the rotational motion of the sled. However, it is unlikely that by reproducing the speed required to simulate an AEB pulse we would reach the wheels' position showed in Figure 6 (right). In any case, our design may support future sled applications that may requires higher rotational speeds.

This study is a work in progress and future dissemination will include the development and improvement of the occupant compartment upon previous iterations of this sled (Griffith et al., 2020).

CONCLUSIONS

The three design criteria assessed for the development of a rotational sled capable of reproducing the acceleration profile of a realistic AEB pulse demonstrates the feasibility of our approach.

ACKNOWLEDGEMENTS

The authors are grateful to the following individuals for their contribution to the design, construction, and installation of the centrifuge sled: Andrew King (Neuma LLC), David Fry (A Service Company Inc.), Madeleine Griffith, Kavan Rajapaksha, Janet Le, Drexel University College of Engineering Machine Shop staff and Dr. Giovanni Savino for suggesting the design of a mathematical model for our sled. The authors are also grateful to the Collaborative Safety Research Center at Toyota Motor Corporation for funding previous developments of this work.

REFERENCES

ARBOGAST, K. B., BALASUBRAMANIAN, S., SEACRIST, T., MALTESE, M. R., GARCIA-ESPANA, J. F., HOPELY, T., CONSTANS, E., LOPEZ-VALDES, F. J., KENT, R. W., & TANJI, H. (2009). Comparison of kinematic responses of the head and spine for children and adults in low-speed frontal sled tests.

CHAN, H., ALBERT, D. L., GAYZIK, F. S., & KEMPER, A. R. (2022). Occupant kinematics of braced 5th percentile female and 50th percentile male volunteers in low-speed frontal and frontal-oblique sled tests. Porto, Portugal: International Research Council on Biomechanics of Injury IRCOBI.

This paper is a student paper from the 20th Injury Biomechanics Symposium and is published in a special issue of SAE International Journal of Transportation Safety.
It is preliminary work, has not been peer reviewed, and should not be cited because it is a work in progress.

CICCHINO, J. B., & ZUBY, D. S. (2019). Characteristics of rear-end crashes involving passenger vehicles with automatic emergency braking. Traffic Injury Prevention, 20(sup1), S112-S118.

GRACI, V., MALTENFORT, M., SCHNEIDER, M., GRIFFITH, M., SEACRIST, T., & ARBOGAST, K. (2021). Quantitative characterization of AEB pulses across the modern fleet. Traffic Injury Prevention, 22(sup1), S62-S67.

GRIFFITH, M., SEACRIST, T., JORDAN, A., SHERONY, R., HALLMAN, J., ARBOGAST, K. B., GRACI, V. (2020). A novel methodology to examine occupant motion during the AEB pulses present in the modern fleet. NHTSA Bio workshop 2020.

HOLT, C., SEACRIST, T., DOUGLAS, E., GRACI, V., KERRIGAN, J., KENT, R., BALASUBRAMANIAN, S., & ARBOGAST, K. B. (2020). The effect of vehicle countermeasures and age on human volunteer kinematics during evasive swerving events. Traffic Injury Prevention, 21(1), 48-54.

INSURANCE INSTITUTE FOR HIGHWAY SAFETY (IIHS) VEHICLE-TO-VEHICLE FRONT CRASH PREVENTION 2.0 TEST PROTOCOL VERSION 1 (APRIL 2024). Url:https://www.iihs.org/media/6462f0aa-75d4-4d94-9170-44b65ab891d7/c9i-JA/Ratings/Protocols/current/FCP%202.0%20test%20protocol%20v1.pdf .

KANG, M., LEE, I., JUNG, J., KIM, S., CHO, Y., KIM, H., & LIM, D. (2021). Motion responses by occupants in out-of-seat positions during autonomous emergency braking. Annals of Biomedical Engineering, 49(9), 2468-2480.

KLUG, C., GREGOR, G. (2024). Analysis of occupant motion in pre-crash AEB manuevers in current and future seating positions. RCCADS public workshop 2024.

SONI, A., SCHILLING, S., & LUCHT, A. (2023). Investigating the Effects of Pre-Pretensioning on Occupant Kinematics and Abdominal Organ Response during Pre-Crash and In-Crash. IRCOBI conference 2023.

This paper is a student paper from the 20th Injury Biomechanics Symposium and is published in a special issue of SAE International Journal of Transportation Safety.
It is preliminary work, has not been peer reviewed, and should not be cited because it is a work in progress.